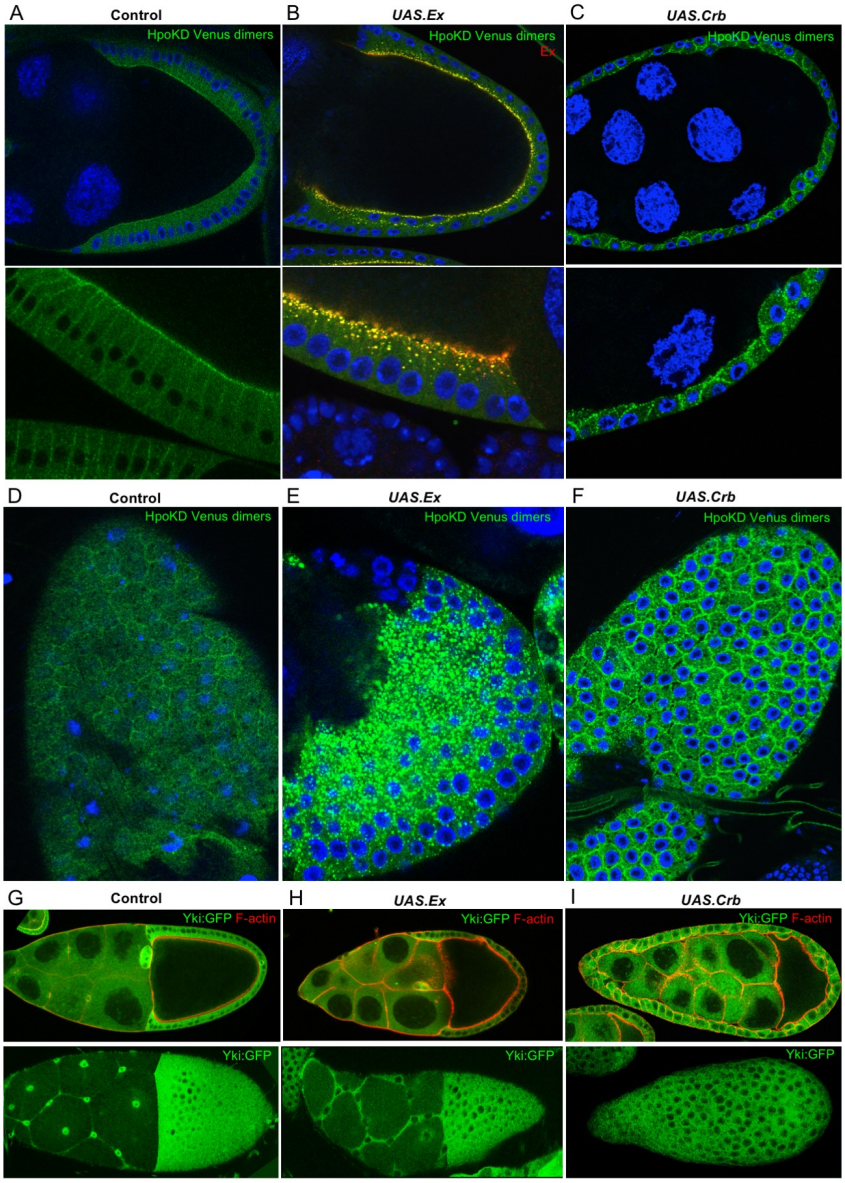

Figure S1. Ectopic induction of Hippo dimerisation and signalling to Yki upon overexpression of Expanded or Crumbs.
(A, D) Expression of split-Venus Hippo dimerisation sensor in the follicular epithelium reveals strong apical activation in columnar follicle cells.
(B, E) Overexpression of Expanded further induces Hippo-Venus dimerisation and induces internalisation into punctae.
(C, F) Overexpression of Crumbs further induces Hippo-Venus dimerisation and induces spreading of Hippo complexes around the plasma membrane due to an expansion of the apical domain.
(G) Yki:GFP in a control stage 10 egg chamber
(H) Yki:GFP in a stage 10 egg chamber expressing *UAS.Ex* under *TJ.Gal4.*
(I) Yki:GFP in a stage 10 egg chamber expressing *UAS.Crb* under *TJ.Gal4*.

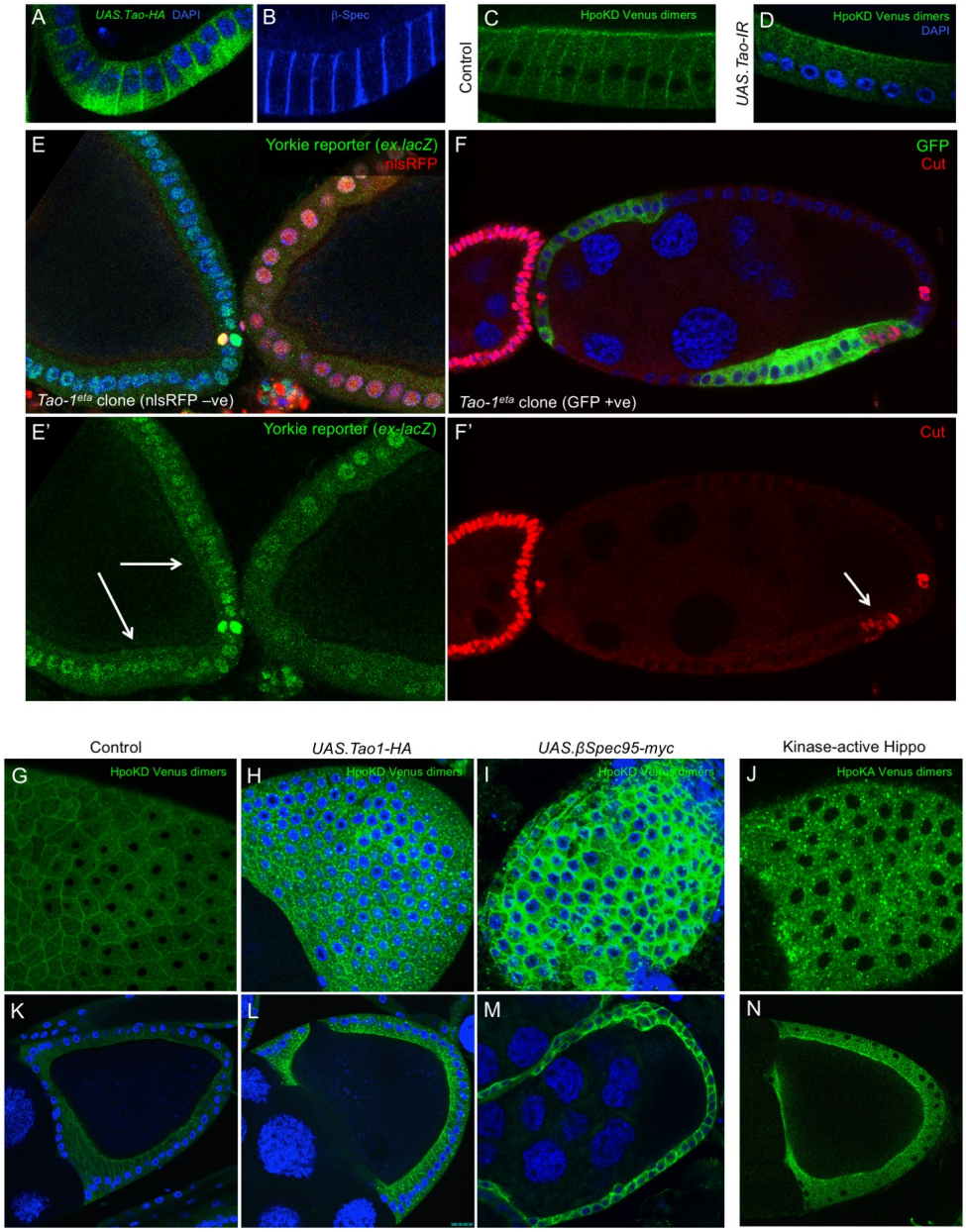

Figure S2. Tao-1 localises laterally with beta-Spectrin to activate Hippo dimerisation and help repress Yorkie target genes in posterior follicle cells.
(A,B) HA-tagged Tao-1 localises laterally with beta-Spectrin in columnar follicle cells.
(C,D) Silencing of Tao-1 by expression of *UAS.Tao1-RNAi* with the *GR1.Gal4* driver causes a reduction in lateral Hippo-Venus dimerisation signal, without affecting the apical signal.
(E) Mutation of Tao-1 in clones marked by the absence of nuclear RFP (red) lead to increased levels of *ex.lacZ* expression in columnar follicle cells.
(F) Mutation of Tao-1 in clones marked by the presence of cytoplasmic GFP (green) lead to increased levels of Cut expression in the posterior-most columnar follicle cells.
(G-N) Overexpression of Tao-1, beta-Spectrin, or kinase-active Hippo-Venus reporter further induces Hippo-Venus dimerisation at either the plasma membrane or intracellular punctae.

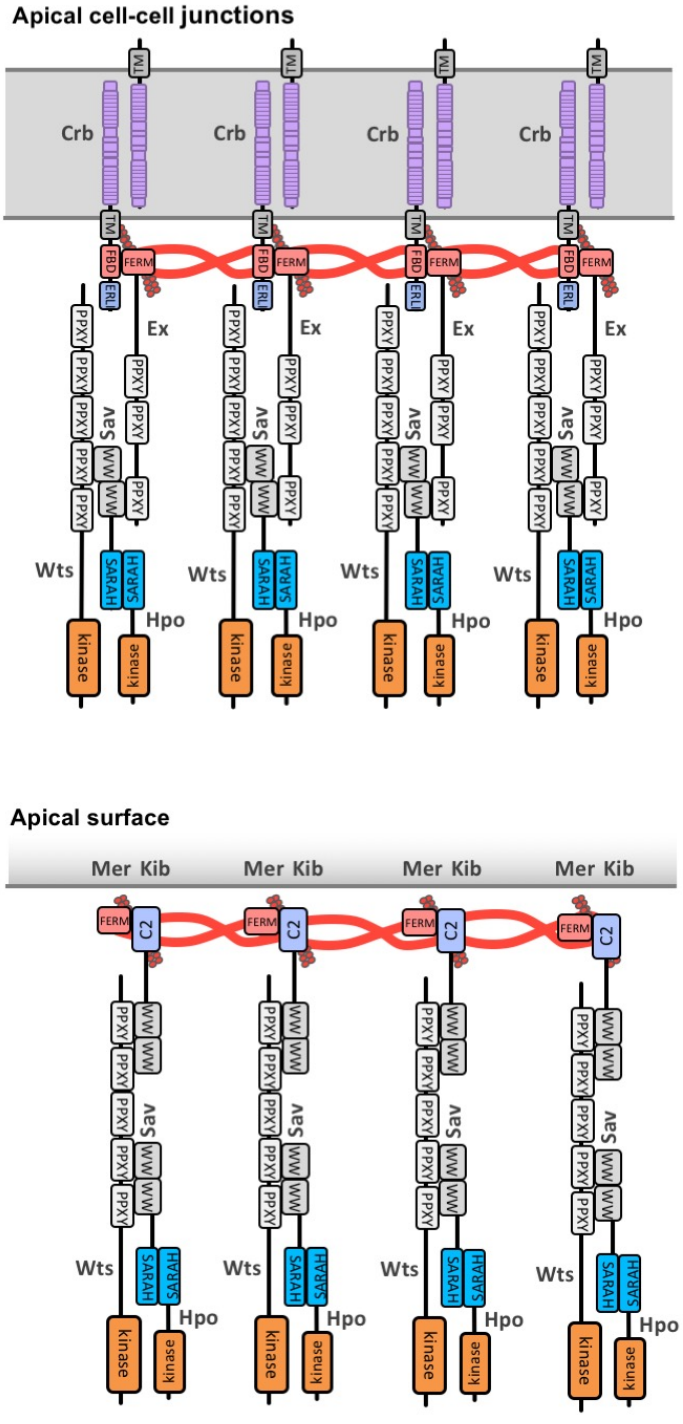

Figure S3. Both apical-junctional Crb-Ex and apical-medial Mer-Kib complexes contribute to Hippo pathway regulation in follicle cells.
Schematic model showing two pools of Hippo kinase regulation, one at the apical junction mediated by Crb and Ex and the other one at the apical-medial surface mediated by Mer and Kib.

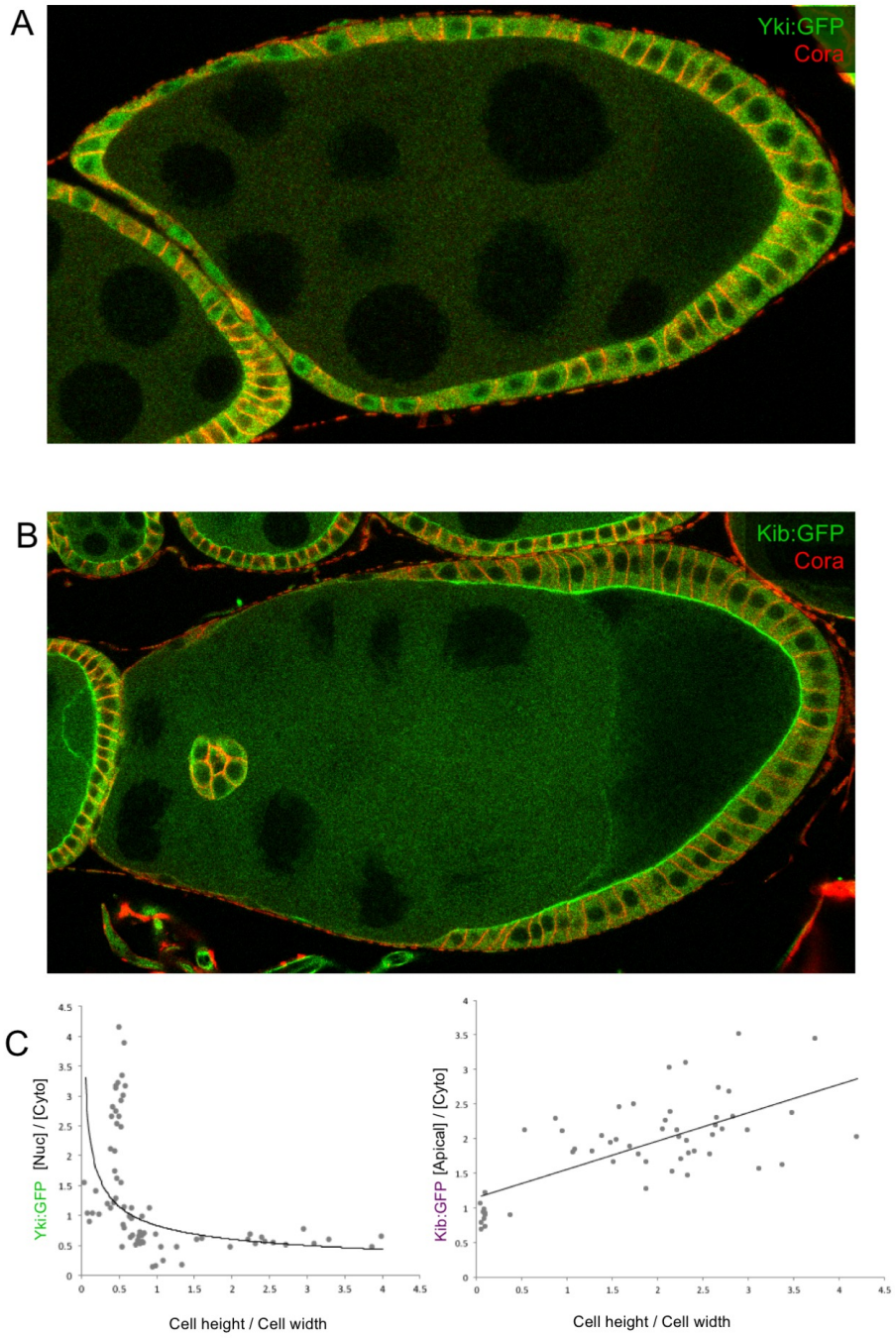

Figure S4. Quantification reveals an exponential increase in Yki nuclear localisation upon linear dilution of the apical Hippo pathway component Kibra in stretch cells.
(A) Stage 9 egg chamber expressing Yki:GFP. Coracle in red marks the lateral membrane. Dapi staining is shown in blue.
(B) Stage 9 egg chamber expressing Kib:GFP. Coracle in red marks the lateral membrane. Dapi staining is shown in blue.
(C) Quantification of nuclear:cytoplasmic ratio of Yki:GFP (n=72) and apical:cytoplasmic ratio of Kib:GFP (n=55) plotted against cell height relative to cell width.

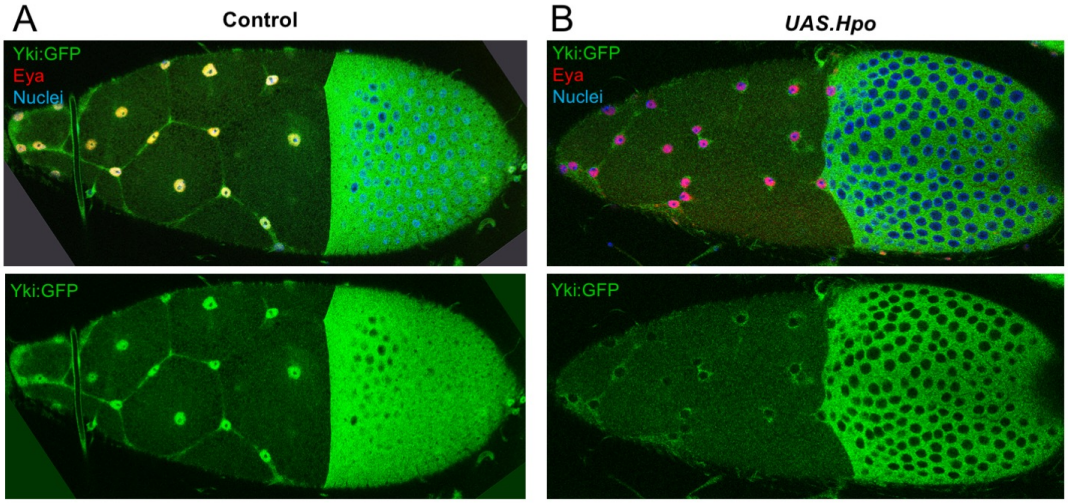

Figure S5. Hippo activation and loss of nuclear Yki does not affect stretch cell fate specification, as measured by expression of the Eyes-absent (Eya) transcription factor.
(A) Control stage 10 egg chamber expressing Yki:GFP (green) and stained for Eya (red) and Dapi (blue).
(B) TJ.Gal4 expressing *UAS.Hpo* results in loss of nuclear Yki:GFP (green) but does not affect Eya (red).

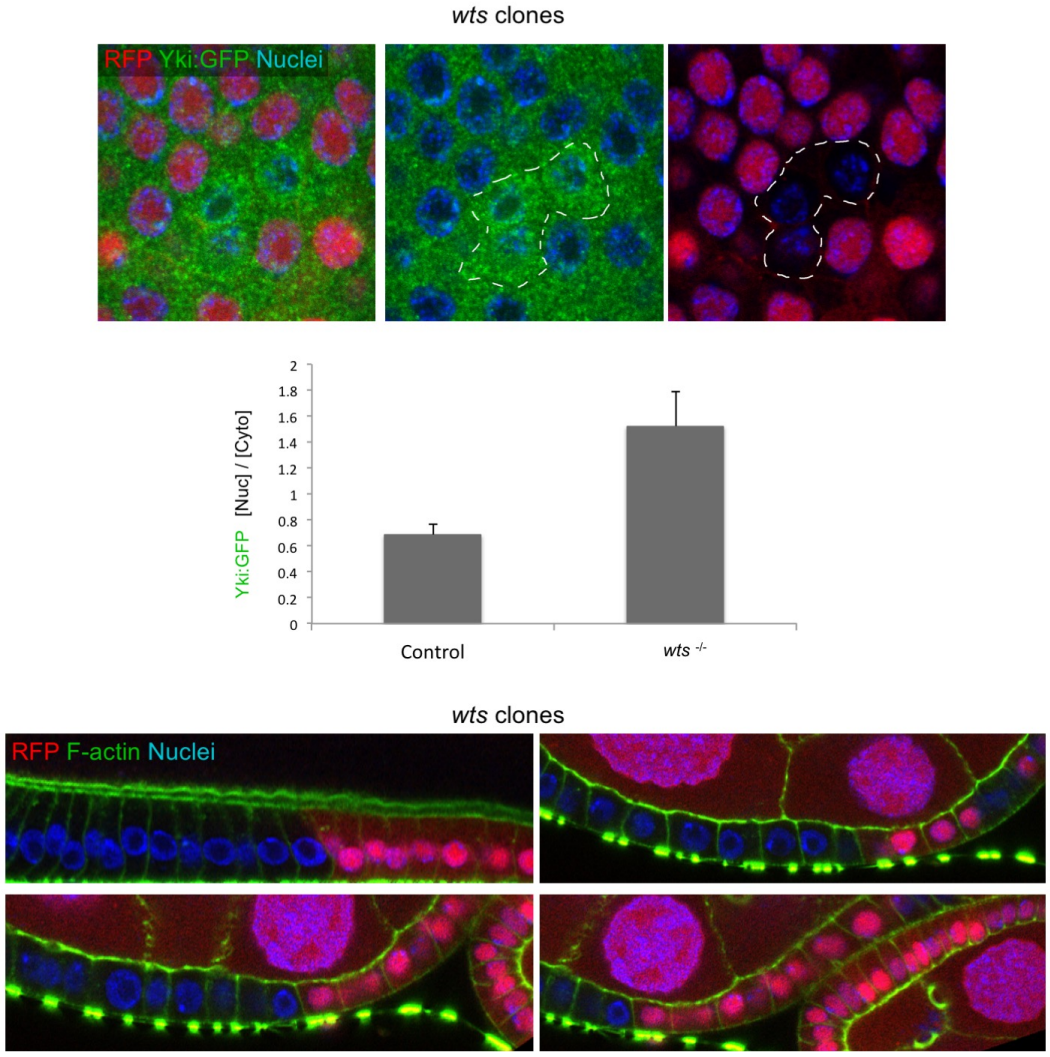

Figure S6: *wts* clones induce nuclear Yki:GFP but do not affect positioning of the nucleus. Quantification of nuclear:cytoplasmic ratio of Yki:GFP in *wts* clones (top; RFP negative cells, n=6). Average and standard deviation (error bars) are represented. Cross sections through different stage egg chambers containing *wts* clones showing that nuclear positioning (DAPI, blue) does not change (bottom).

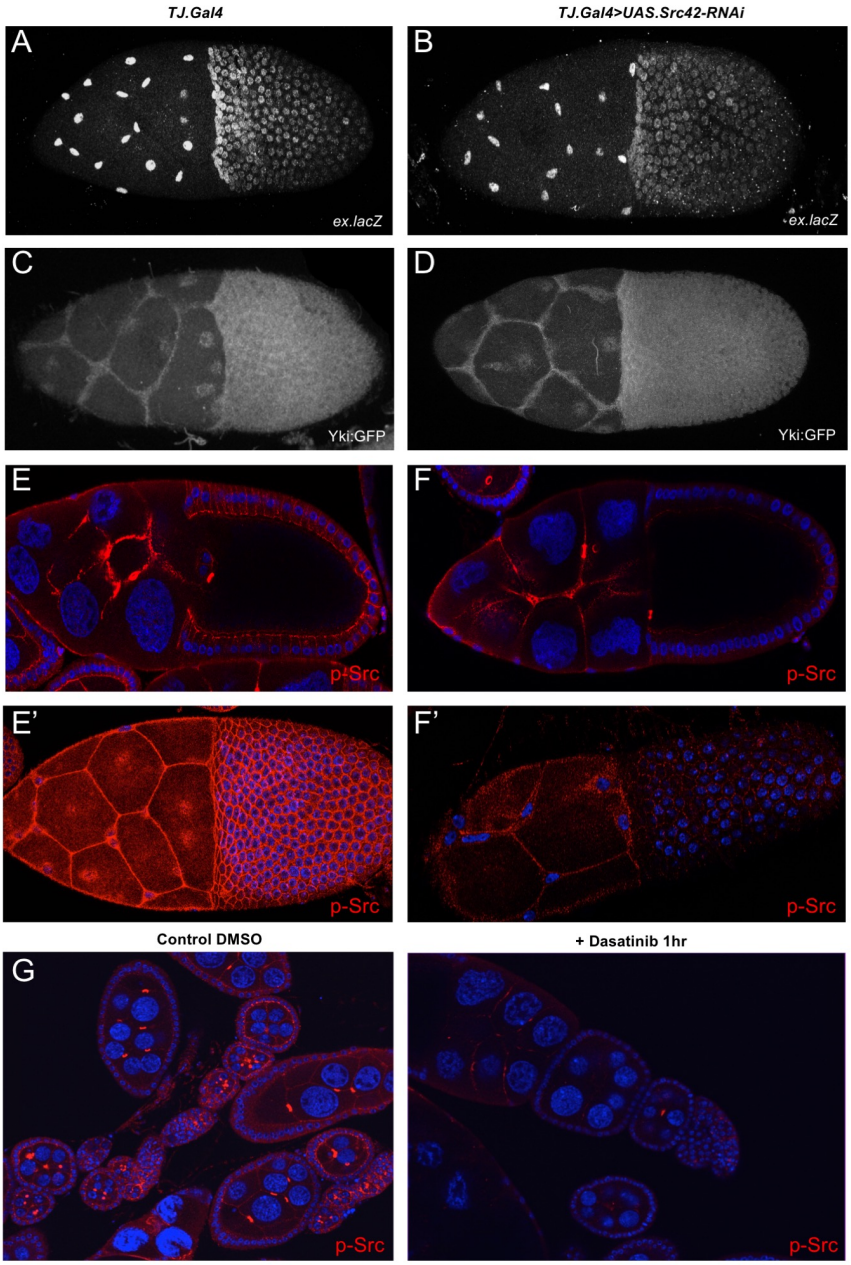

Figure S7. Inhibition of Src with RNAi or Dasatanib treatment reduces p-Src levels but does not affect Yki:GFP localisation or ex.lacZ expression.
(A) Control stage 10 *Ex.LacZ* egg chamber
(B) Silencing of Src42a by *UAS.RNAi* hairpin expression with TJ.Gal4 driver does not reduce expression of ex.lacZ in stretch cells.
(C) Control stage 10 Yki:GFP egg chamber
(D) Silencing of Src42a by *UAS.RNAi* hairpin expression with TJ.Gal4 driver does not reduce nuclear localisation Yki:GFP in stretch cells.
(E,F) Cross-section and apical views of phospho-Src staining shows the reduction in active Src levels upon *Src42a-RNAi*.
(G) Dasatinib is an effective inhibitor of Src activity as measured by autophosphorylation.

Dapi staining is shown in blue.

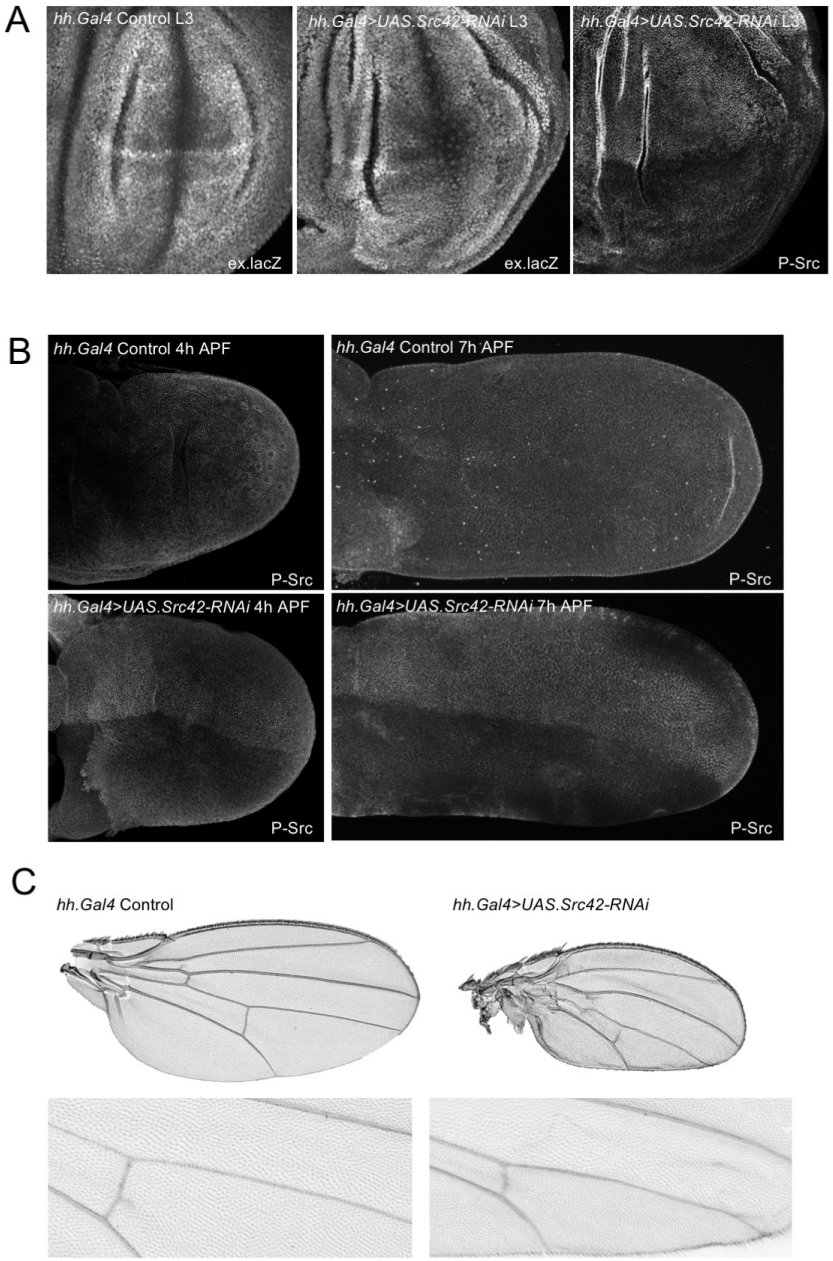

Figure S8. Src42 RNAi does not affect Yki target gene expression but does reduce cell size in the wing, indicating a Hippo pathway independent function.
(A) Silencing of Src42 by *UAS.RNAi* hairpin expression with *Hedgehog-Gal4* (*hh.Gal4*) driver does not reduce expression of ex.lacZ in the wing imaginal disc.
(B,C) Silencing of Src42 by *UAS.RNAi* hairpin expression with *hh.Gal4* driver reduces posterior compartment size and cell size (revealed by increased hair density) adult wings.

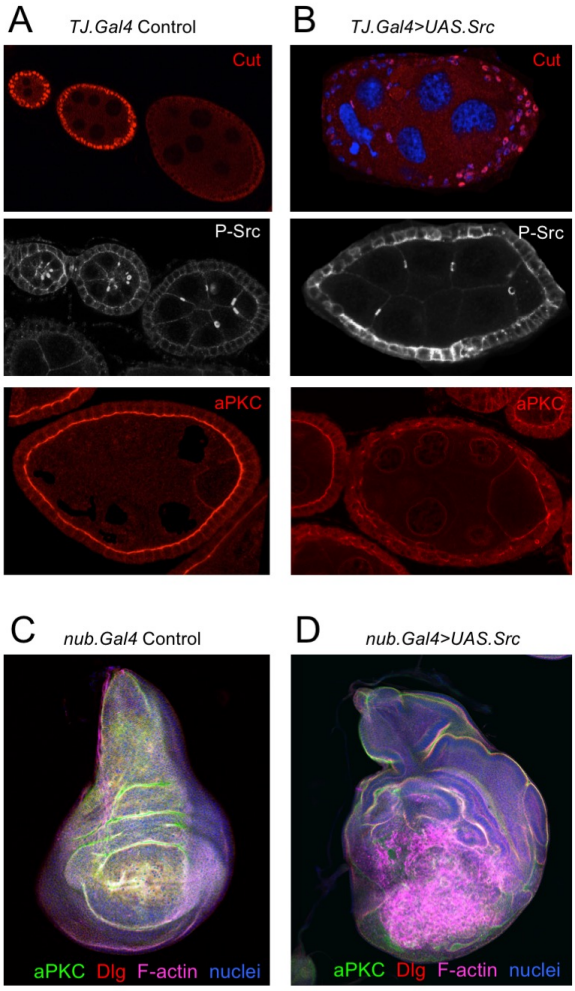

Figure S9. Overexpression of Src indirectly affects Yki target gene expression via alterations in epithelial cell polarity.
(A,B) Overexpression of *UAS.Src* with the *TJ.Gal4* driver induces expression of the Yki target gene Cut, but also disrupts the apical domain of follicle cells at stage 8 of oogenesis.
(C,D) Overexpression of *UAS.Src* with the nubbin.Gal4 (nub.Gal4) driver disrupts epithelial cell polarity in the wing imaginal disc, suggesting an indirect effect of Src overexpression on Yki.

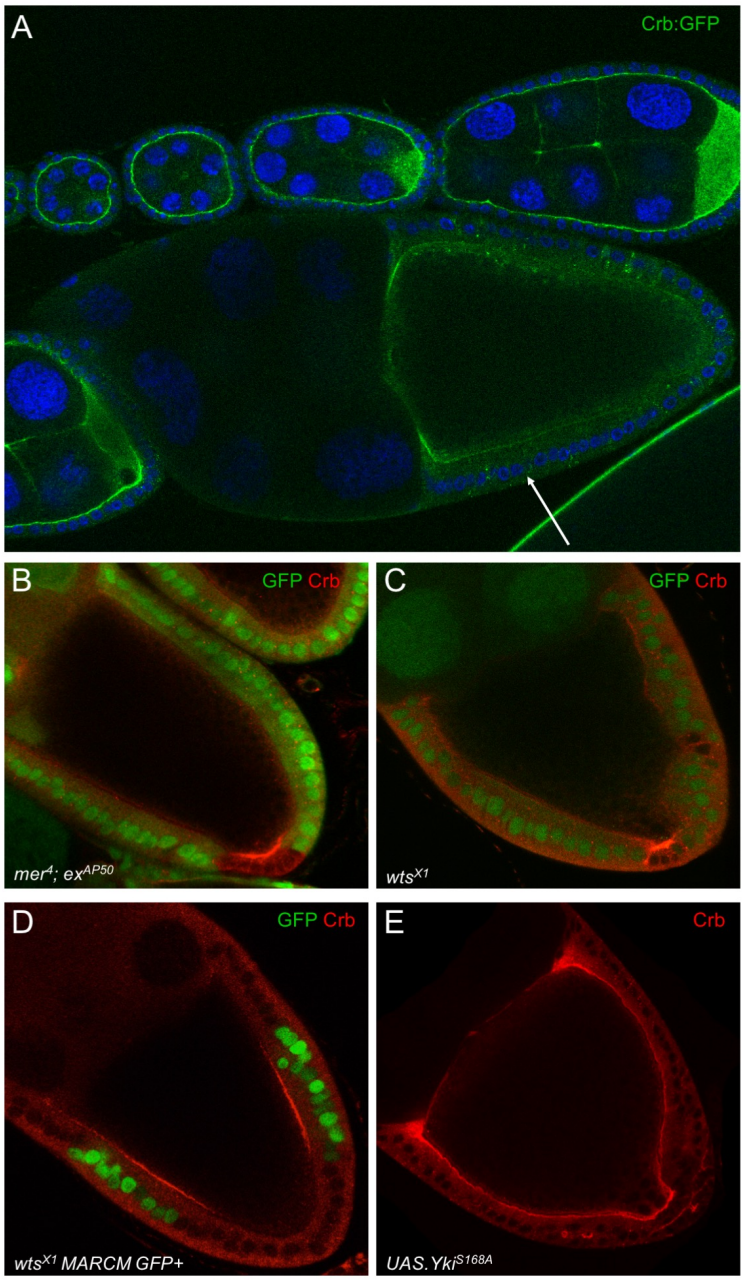

Figure S10. Activation of Hippo signalling in columnar cells at stage 10 of oogenesis downregulates Crb in a negative feedback loop.
(A) Crb:GFP is strongly expressed at the apical membrane of follicle cells prior to stage 10 after which it becomes clearly down-regulated.
(B) *mer, ex* double clones (GFP negative) have increased levels of Crb at the apical membrane.
(C) *wts* clones (GFP negative) have increased levels of Crb at the apical membrane.
(D) *wts* clones (GFP positive) have increased levels of Crb at the apical membrane.
(E) *TJ.Gal4, UAS-Yki*^{S168A} expressing stage 10 egg chamber in which Crb remains at the apical membrane in all follicle cells.

Table S1. *Drosophila* genotypes

Fig S1A, D: *TJ.Gal4, UAS.Hippo$^{Kinase\text{-}dead}$VenusC; UAS.Hippo$^{Kinase\text{-}dead}$VenusN/+*
Fig S1B, E: *TJ.Gal4, UAS.Hippo$^{Kinase\text{-}dead}$VenusC; UAS.Hippo$^{Kinase\text{-}dead}$VenusN/UAS-Ex; +*
Fig S1C, F: *TJ.Gal4, UAS.Hippo$^{Kinase\text{-}dead}$VenusC; UAS.Hippo$^{Kinase\text{-}dead}$VenusN/UAS-Crb; +*
Fig S1G: *GR1.Gal4, Yki:GFP/+*
Fig S1H: *GR1.Gal4, Yki:GFP/UAS.Ex*
Fig S1I: *GR1.Gal4, Yki:GFP/UAS.Crb*

Fig S2A: *TJ.Gal4/UAS.Tao-HA* (Gomez et al., 2012)
Fig S2B: *TJ.Gal4/UAS.Tao-HA*
Fig S2C: *TJ.Gal4, UAS.Hippo$^{Kinase\text{-}dead}$VenusC; UAS.Hippo$^{Kinase\text{-}dead}$VenusN/+*
Fig S2D: *TJ.Gal4, UAS.Hippo$^{Kinase\text{-}dead}$VenusC; UAS.Hippo$^{Kinase\text{-}dead}$VenusN/+; UAS.TaoIR (VDRC KK107645)*
Fig S2E: *hs.flp, frt19a ubiRFPnls/Tao^{eta}19a; ex^{lacz}/+*
Fig S2F: *hs.flp, frt19a ubiRFPnls/Tao^{eta}19a*
Fig S2G: *TJ.Gal4, UAS.Hippo$^{Kinase\text{-}dead}$VenusC; UAS.Hippo$^{Kinase\text{-}dead}$VenusN/+*
Fig S2H: *TJ.Gal4, UAS.Hippo$^{Kinase\text{-}dead}$VenusC; UAS.Hippo$^{Kinase\text{-}dead}$VenusN/UAS.Tao-HA; +*
Fig S2I: *TJ.Gal4, UAS.Hippo$^{Kinase\text{-}dead}$VenusC; UAS.Hippo$^{Kinase\text{-}dead}$VenusN/UAS.βSpec95-myc* (Mazock et al., 2010)
Fig S2J: *TJ.Gal4, UAS.Hippo$^{Kinase\text{-}active}$VenusC; UAS.Hippo$^{Kinase\text{-}active}$VenusN/+*
Fig S2K: *TJ.Gal4, UAS.Hippo$^{Kinase\text{-}dead}$VenusC; UAS.Hippo$^{Kinase\text{-}dead}$VenusN/+*
Fig S2L: *TJ.Gal4, UAS.Hippo$^{Kinase\text{-}dead}$VenusC; UAS.Hippo$^{Kinase\text{-}dead}$VenusN/UAS.Tao-HA; +*
Fig S2M: *TJ.Gal4, UAS.Hippo$^{Kinase\text{-}dead}$VenusC; UAS.Hippo$^{Kinase\text{-}dead}$VenusN/UAS.βSpec95-myc (Mazock et al., 2010)*
Fig S2N: *TJ.Gal4, UAS.Hippo$^{Kinase\text{-}active}$VenusC; UAS.Hippo$^{Kinase\text{-}active}$VenusN/+*

Fig S4A: *Yki:GFP*
Fig S4B: *Kib:GFP*

Fig S5A: *TJ.Gal4, Yki:GFP /+*
Fig S5B: *TJ.Gal4, Yki:GFP /UAS-Hippo*

Fig S6: *hsflp/+; Yki:GFP / Yki:GFP; wtsXI 82B/82B GFP*

Fig S7A: *ex-LacZ, TJ.Gal4/+*
Fig S7B: *ex-LacZ TJ.Gal4/+ UAS-Src42a.IR (VDRC 26019)/+*
Fig S7C: *Yki:GFP , TJ.Gal4/+*
Fig S7D: *Yki:GFP, TJ.Gal4/+; UAS-Src42a.IR (VDRC 26019)/+*
Fig S7E, E': *TJ.Gal4*
Fig S7F, F': *TJ.Gal4/+ UAS-Src42a.IR (VDRC 26019)/+*
Fig S7G: *W^{iso}*

Fig S8A: *ex-LacZ; Hh.G4/+* and *ex-LacZ; Hh.G4/UAS-Src42a.IR*
Fig S8B: *Hh.G4/+* and *Hh.G4/UAS-Src42a.IR*
Fig S8C: *Hh.G4/+* and *Hh.G4/UAS-Src42a.IR*

Fig S9A: *TJ.Gal4/+*
Fig S9B: *TJ.Gal4/UAS.Src64b*
Fig S9C: *Nub.G4/+*
Fig S9D: *Nub.G4/UAS.Src64b*

Fig S10A: *Crb:GFP*
Fig S10B: *hsflp 19a GFP/19a* mer^{4}, ex^{AP50}
Fig S10C: *hsflp;; FRT82B* wts^{XI}*/FRT82B GFP*
Fig S10D: *yw TubGAL4 hsFLP 122 UAS-nucGFPmyc;; FRT82B CD21 y+ TubG80.LL3/FRT82B* wts^{XI}
Fig S10E: *TJ.Gal4/UAS-*Yki^{S168A}*; Crb:GFP/+*

References

Gomez, J. M., Wang, Y. and Riechmann, V. (2012). Tao controls epithelial morphogenesis by promoting Fasciclin 2 endocytosis. *J Cell Biol* **199**, 1131-1143.

Mazock, G. H., Das, A., Base, C. and Dubreuil, R. R. (2010). Transgene rescue identifies an essential function for Drosophila beta spectrin in the nervous system and a selective requirement for ankyrin-2-binding activity. *Mol Biol Cell* **21**, 2860-2868.